International Journal of Chemistry Studies
www.chemistryjournal.in
ISSN: 2581-348X
Received: 19-08-2024, Accepted: 18-09-2024, Published: 03-10-2024
Volume 8, Issue 2, 2024, Page No. 35-40

Metal oxide nanoparticles using biological and electrochemical techniques

Sakshi Mokashi[1], Anil Sharma[2]
[1] Research Scholar, Department of Chemistry, Kalinga University, Raipur, Chhattisgarh, India
[2] Professor, Department of Chemistry, Kalinga, University, Raipur, Chhattisgarh, India

Abstract
This study investigates the optical, electrical, and viscosity properties of polyvinyl alcohol (PVA) films embedded with chromium oxide (Cr_2O_3) nanoparticles, aiming to explore their potential applications in advanced materials. PVA films were synthesized through a solution casting method, incorporating varying concentrations of Cr_2O_3 nanoparticles to evaluate their effects on the material's properties. UV-Vis spectroscopy was used to analyze the optical properties, revealing a significant reduction in optical transmittance with increasing nanoparticle concentration, indicative of enhanced light absorption. Electrical conductivity was measured using a four-point probe method, showing an improvement in conductivity as Cr_2O_3 content increased, attributed to the semiconducting nature of the nanoparticles. The viscosity of the PVA-nanoparticle solution was measured, demonstrating that the addition of Cr_2O_3 increases the viscosity, which can be linked to the interaction between PVA chains and nanoparticles. The interplay between the optical, electrical, and viscosity properties of the nanocomposite films suggests promising applications in optoelectronic devices, sensors, and nanocomposite materials with tunable properties.

Keywords: Metal oxide nanoparticles, biological techniques, electrochemical techniques

Introduction

Nanotechnology has become a vital area of study in the biomedical sciences over time. This is a result of the most recent bioengineering techniques, which make it possible to manipulate created nanomaterials easily [1]. Compared to larger particles, nanoparticles (NPs) are used extensively as materials in the tissue engineering, pharmaceutical, and cosmetics industries because of their special qualities, which include physiochemical stability, increased surface area, biocompatibility, and non-toxicity [2].

Metal and oxide nanoparticles (NPs) are the most researched material groups. Several studies have demonstrated the significant therapeutic benefits of metal nanoparticles (NPs) (Cu, Ag, Pt, Au, Pt, Mg, Zn, etc.) and metal oxides (ZnO, TiO2, CuO, Ag2O, etc.). Because of these advantages, they are being used in many different domains, including biosensors, drug delivery systems, tissue engineering scaffolds, and diagnostic imaging applications [3, 4].

Chemical and physical techniques represent the main routes for the synthesis of metal and metal oxide nanoparticles (NPs). Precipitation, the sol-gel method, chemical reduction, and polyol synthesis are the most studied chemical synthesis routes; on the other hand, evidence of microwave-assisted combustion, laser evaporation, and pulsed laser deposition was found for physical synthesis routes [5, 6].

These techniques do have several drawbacks, though, including the use of hazardous materials, inefficiency in terms of cost, the use of risky processes, and the creation of hazardous byproducts that are bad for the environment. The intricate processes and disadvantages associated with the aforementioned synthesis routes compromise the biocompatibility of nanoparticles. Therefore, the development of an economical, one-step, dependable, biocompatible, and non-toxic method for the synthesis of environmentally friendly nanoparticles is urgently needed. One line of inquiry employs biological techniques involving the use of microorganisms, plant extracts, and enzymes [6, 7].

By substituting eco-friendly metabolites and biomolecules inspired by synthesis routes like biomimetic or biological synthesis, the steps taken in green synthesis methods for metallic NPs aim to reduce or eliminate the use of toxic substances and solvents [8].

The use of metallic and metal oxide nanoparticles (NPs) in tissue engineering has increased, particularly because of their antibacterial qualities [9, 10].

NPs have been applied in this direction to support various functions in tissue engineering, including DNA transfection, gene delivery, cell patterning, and viral transduction, in addition to improving mechanical, electrical, and biological properties. NPs' primary functions are to support the development of various tissue types or to aid in molecular detection or biosensing. Additionally, depending on the intended application, the use of NPs in tissue engineering can both improve and add properties to the scaffolds. Due to their small size and correlation with a high surface-to-volume ratio, the extra properties are provided. As a result, the NPs can readily diffuse across membranes, which promotes cell uptake. Furthermore, NPs can replicate the dimensions of extracellular matrix elements in native tissues [11, 12, 13, 14].

High control over the properties of the resulting scaffolds, such as maximising their mechanical strength and providing the potential for controlled release of bioactive agents, is another crucial feature of metal nanoparticles [15]. Despite the fact that numerous studies found that metal nanoparticles (NPs) were more toxic, more recent studies have shown that the right dosage, size, and distribution of the materials can actually lower their toxicity. The primary characteristics of these materials could be enhanced to produce a more effective therapeutic effect because of their nature and ease of functionalisation [16, 17]. Their optimization's primary objective was to create specific conditions in order to pursue the mechanical and biological properties that would make them perfect materials for the intended use. In order to overcome the primary obstacles in

tissue engineering, the developed NPs offer high surface area and adjustable surface properties, enhancing the scaffolds' mechanical strength, antiseptic properties, and antibacterial activity. Numerous metal/metal oxide nanoparticles have been used up to this point to alter and enhance the functionality of scaffolds. In many cases, the scaffolds incorporate polymers along with ceramic, polymeric, and other NPs [14, 15, 18].

In addition, nanoparticles have the capacity to regenerate wounds and display antimicrobial qualities, which makes them special materials that may facilitate wound healing. Due to their excellent efficacy and environmental friendliness, green synthesised NPs have drawn more attention in this direction, making the produced material promising for use as wound healing agents [19]. Furthermore, because of their antimicrobial, antioxidant, antibacterial, anticancerous, and antiviral activity, Mujahid *et al.* [20] verified the effective use of metal and metal oxide NPs in drug delivery applications. Thus, the mechanism of nanoparticles' antimicrobial activity is depicted in Figure 1. This mechanism offers a viable path to circumvent antibiotic resistance, antibiotic modification, and biofilm formation inactivation.

Method and material

Experimental

Two distinct methods for electrochemically synthesizing chromium oxide nanoparticles are explored, and the results of these generated nanoparticles are compared.

Method 1 (Electrochemical method in presence of $K_2Cr_2O_7$andH_2SO_4)

It is possible to electrochemically synthesize chromium oxide nanoparticles using platinum electrodes. Twenty milliliters of potassium dichromate solution and five milliliters of concentrated sulfuric acid (conc.H_2SO_4) were used in the experiment. The Neulite India battery eliminator was used to provide a positive 12V at a usable current of 70 mA to 90 mA. The experiment was run for three hours while being continuously stirred. The orange color gradually faded into a dark green one. During two hours at a temperature of 1,000 degrees Celsius, the aforesaid solution was allowed to evaporate slowly. The sulphate test was positive for the dried substance that was collected. In addition, moisture and sulfate as sulfur dioxide were removed by calcining the material at temperatures between 6500C and 7000C.

Method 2 (In thepresenceof (Pt/Cr) and $NaHCO_3$ Electrochemical method)

This technique included electrochemically depositing a thin layer of chromium from chromium nitrate solution onto a platinum electrode (Pt/Cr) (0.1M). A 20 ml NaHCO3 solution was used in a reaction chamber for the synthesis of Cr_2O_3 nanoparticles. Power was supplied at 12V with 30 mA flowing via a Pt/Cr anode and a Pt cathode. Three hours passed during which time the experiment was done with continual stirring and temperature. Scheme 3.2 depicts the electrochemical reaction between Cr^{3+} ions (obtained via the anodic dissolution of chromium) and aqueous $NaHCO_3$ (used to generate Cr3+ oxides/hydroxides). The synthesis occurs at the electric double layer or at the contact between the electrodes. After filtering out any unreacted NaHCO3, rinsing the gel with distilled water, and drying it at 100 °C to eliminate moisture and hydroxides, the final product was able to float in the electrolyte solution.

Result and discussion

Several methods were used to characterize the chromium oxide nanoparticles. The (ELICO SL171) double beam spectrophotometer was used to take the UV-Visible readings. The Fourier-transform infrared spectrometer was used to capture spectra from 4000 to 400 cm^{-1}. The morphological properties of the Cr2O3 nanoparticles were analyzed using scanning electron microscopy (SEM) and an X-ray diffraction (XRD) pattern generated by a pananalytical X-ray diffractometer utilizing CuK radiation (λ=1.5406A^0).

- **UV-Visiblespectra**

It is suggested that the material may become photoactive in response to visible light since the picture displays maximum absorption at 430 nm, which is typical for Cr2O3 according to the literature.

Table 1: Absorbance ofCr_2O_3nanoparticles

A=2-logT	λnm
1.269	360
1.362	370
1.419	380
1.315	390
1.118	400
1.214	410
1.273	420
1.214	430
0.976	440
0.685	450
0.398	460
0.207	470
0.101	480
0.046	490
0.020	500
0.011	510
0.007	520
0.006	530
0.006	540
0.005	550
0.005	560
0.005	570

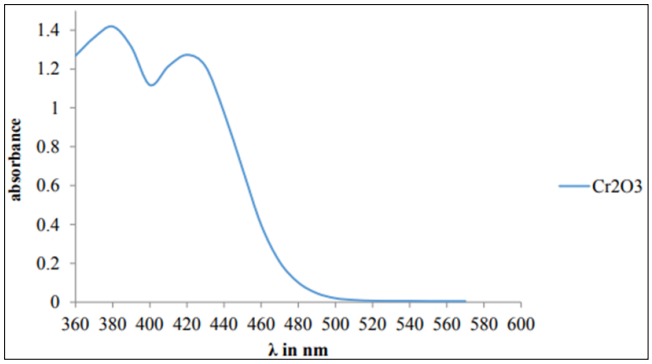

Fig 1: UV-Vis absorption spectrum of Cr2O3 nanoparticles in aqueous solution

- **Infraredspectra**

Chromium oxide nanoparticles generated using electrochemical methods 1 and 2 are shown in figures, together with their respective infrared (IR) spectra. Metal

oxides often exhibit absorption bands at 967 cm-11037 cm^{-1}, 585 cm-1641 cm^{-1}, and 1046 cm-11085 cm^{-1} due to vibrations between their atoms. It has been determined that the frequency ranges for Cr=O vibrations are 967–1037 cm^{1}, Cr–O vibrations are 585–641 cm2, and Cr–O–Cr vibrations are 1046–1085 cm^{2}.

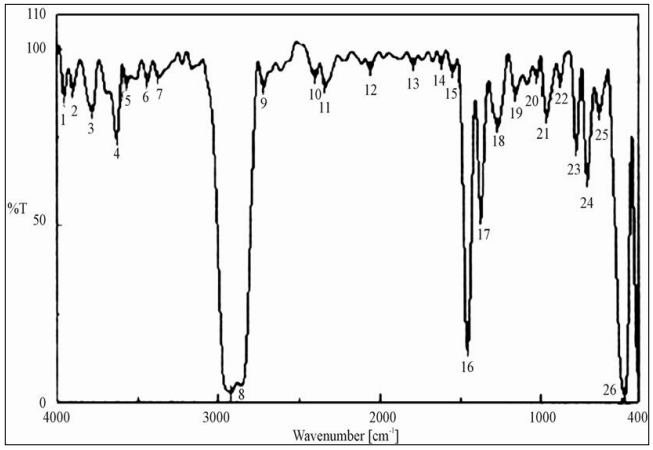

Fig 2: Electrochemically synthesized nanoparticles of Cr_2O_3 in a $K_2Cr_2O_7$ and H_2SO_4 media, as shown in their infrared spectrum

Table 2: IR spectra of Cr_2O_3 nanoparticles synthesized through the electrochemical approach with $K_2Cr_2O_7$ and H_2SO_4 as medium, with selected peaks

Number	Position	Intensity
1	3952.39	86.3835
2	3897.43	88.1084
3	3779.8	82.097
4	3628.41	74.56
5	3586.7	90.3481
6	3439.42	91.0343
7	3370	91.885
8	2922.59	2.7435
9	2722.03	89.3572
10	2402.87	92.1919
11	2341.16	89.463
12	2058.64	94.467
13	1793.47	95.829
14	1617.02	95.982
15	1545.67	93.799
16	1455.99	14.899
17	1372.1	52.289
18	1267.97	78.240
19	1159.01	87.308
20	1047.87	92.175
21	967.126	80.856
22	880.345	91.1
23	783.922	71.546
24	717.39	62.863
25	641.215	81.891
26	584.045	2.053

- **X-raydiffraction**

Chromium oxide nanoparticles synthesized using electrochemical methods 1 and 2 yielded the X-ray diffraction patterns seen in the images. Distinct peaks may be seen in the XRD spectrum.

Both their peak locations and relative intensities are exactly linked to crystalline Cr2O3. Specifically, the (012), (110), (024), and (214) crystal planes of crystalline Cr2O3 are represented by the peaks with 2 values of 24.60, 38.30, 50.020, and 60.620, respectively. Using the Debye-Scherrer equation for all X-ray diffraction peaks, we calculated an average crystalline size, Dhkl.

$$D_{hkl}\,(A0) = \frac{K}{\beta \cos\theta}$$

Where K = shape factor that normally ranges 0.9-1.0 (in our caseK=0.9), λ = X-ray wavelength, & β and θ = half width of the peak and halfof the Bragg angle, respectively. The equation was used to determine that the crystalline sizes of the Cr2O3 nanoparticles generated through electrochemical method 1 were 79 nm and via electrochemical method 2 were 41 nm.

Table 3: Settings for the XRD Instrument's Anchor Scan

ScanAxis	Gonio
AnodeMaterial	Cu
Divergenceslit size	0.500
DivergenceslitType	Fixed
Endposition [2Th]	103.9882
GeneratorSettings	40 mA, 45 kV
Measurementtemperature[^{0}C]	25
PSD Length [2Th]	2.12
PSDmode	Scanning
Scanstep Time[s]	19.6850
ScanType	Continuous
Specimen Length[mm]	10.00
Spinning	Yes
Startposition[2Th]	23.0042
Step Size[2Th]	0.0080

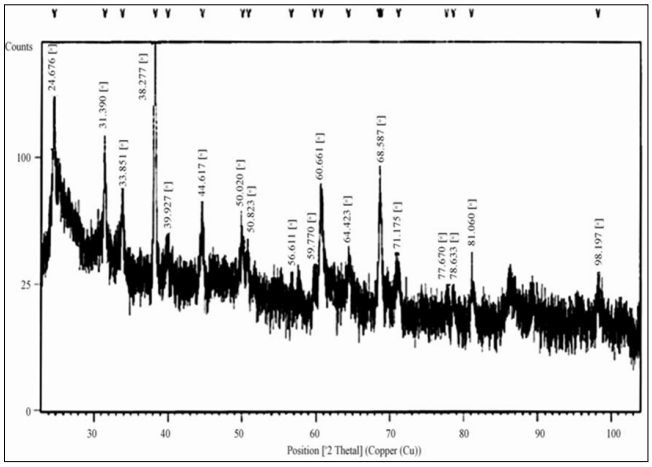

Fig 3: Nanoparticles of Cr2O3 generated using electrochemical means, with K2Cr2O7 and H2SO4 as the medium, as shown in an X-ray powder diffraction pattern

- **SEM**

The photocatalytic activity of photocatalysts are mostly determined by their particle size and surface area. Scanning electron microscopy analysis of Cr2O3 nanoparticles generated using either electrochemical technique 1 or electrochemical method 2 is shown in the images. Little, somewhat agglomerated particles are what the samples indicate.

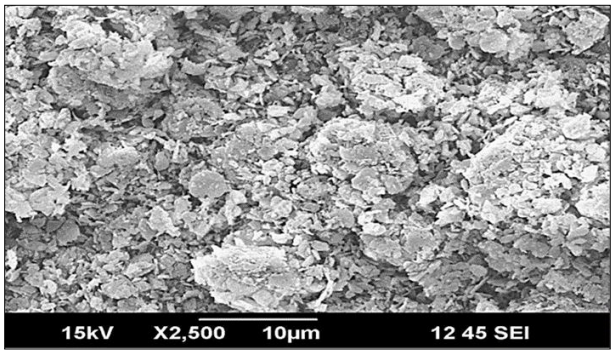

Fig 4: SEM images of Cr_2O_3 nanoparticles synthesized from electrochemical method using K2Cr2O7 and H2SO4 as medium

Chromium oxide role as a catalyst in the breakdown of KMnO4

Chromium oxide nanoparticles, a p-type semiconductor, have been investigated for their potential catalytic effects. By altering both the KMnO4 concentration and the quantity of catalyst, the kinetics of the decomposition reaction has been examined.

Effect of $KMnO_4$ ontherate

The reaction was carried out in three separate beakers containing 10 ml of KMnO4 (0.0001M, 0.00005M, and 0.0002M) with 20.0 mg of Cr2O3 nanoparticles produced through electrochemical technique 1 and method 2. The spectrophotometer was used to track the reaction rate as a function of the changing KMnO4 concentration throughout the room-temperature experiment. Decomposition of KMnO4 occurs more quickly with Method 2 than Method 1, as shown by a plot of log%T vs time. The findings demonstrate that the Cr2O3 nanoparticles generated using procedure 2, with a Cr2O3 size of 41 nm, had extremely high catalytic activity. This suggests that the smaller the size of Cr2O3, the greater the catalytic activity.

Table 4: Decomposition of (0.0001M) $KMnO_4$ by Cr_2O_3 nanoparticles synthesizedfromelectrochemical method 1 and 2

	Time in min												
%Tat 528nmof $KMnO_4$+Cr_2O_3	30	60	90	120	150	180	210	240	270	300	330	360	390
Method1	35.6	45.1	51.2	55.4	57.6	61.6	66.6	71.6	76.0	81.3	85.0	87.0	89.3
Method2	36.1	48.8	56.8	63.0	67.6	72.1	77.8	80.2	84.2	87.0	89.4	92.3	95.1

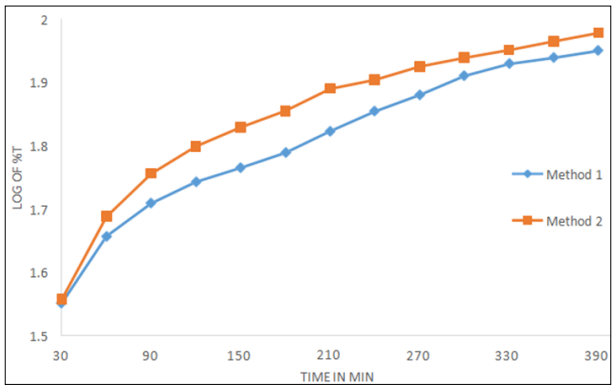

Fig 6: Decomposition kinetics of (0.0001M) $KMnO_4$ by Cr_2O_3 nanoparticles synthesized from electrochemical method 1 and method 2

Effect of Cr_2O_3 nanoparticles on the rate

To investigate the role of the catalyst in the decomposition of KMnO4, a series of experiments were carried out with different concentrations of KMnO4 (1.00104M) and variable quantities of Cr2O3 nanoparticles (10.0 mg, 20.0 mg, and 30.0 mg). The results are shown in tables and figures, and they show that the rate rises with increasing amounts of Cr2O3 nanoparticles. The catalytic activity of Cr2O3 created by electrochemical method 2 was found to be greater than that of Cr2O3 synthesized by electrochemical method 1. When the quantity of catalyst increased, the rate of breakdown decreased. The decreased breakdown rate is due to the fact that, at high concentrations, Cr2O3 particles aggregate, reducing the number of active sites on the surface.

Table 6: (0.0001M) $KMnO_4$ Decomposition by 10.00 mg of Cr_2O_3nanoparticlessyn the sized from electrochemical method1 and 2

	Time in min									
%Tat 528nm of $KMnO_4$+Cr_2O_3	45.0	90.0	135.0	180.0	225.0	270.0	315.0	360.0	405.0	450.0
Method 1	42.3	46.4	49.3	50.9	51.1	52.0	52.8	53.2	53.9	54.1
Method 2	48.7	59.0	70.1	74.2	78.3	81.3	84.5	89.0	90.1	92.3

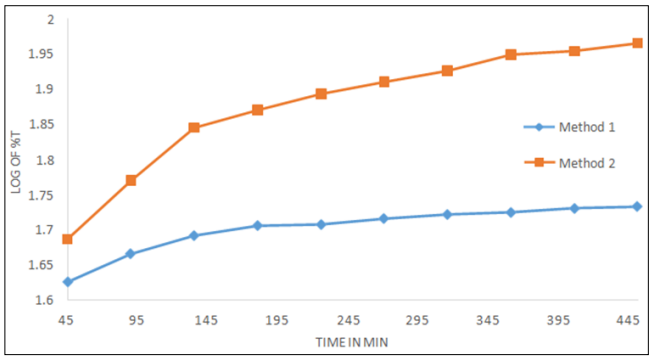

Fig 7: (0.0001M) $KMnO_4$ Decomposition kinetics by 10.00mg Cr_2O_3 nanoparticles synthesized from electrochemical method 1 and 2

Antibacterial Assay

Using the Disc diffusion method, we determined whether or whether Cr2O3 nanoparticles made through electrochemical techniques 1 and 2 were effective at inhibiting the growth of Escherichia coli and Pseudomonas aregunosa. Pure bacterial cultures were separated and propagated in subcultures on nutrient agar. The results were compared to those obtained with regular Gentamycin. The nanoparticle concentration in each solution was 50 mg/ml, and the volume was 50 l. Bacterial zone inhibition was evaluated after 48 hours of incubation at 370C. Table and images depict the milimeter-sized inhibitory zone around Cr2O3 nanoparticles. The table shows that the Cr2O3 nanoparticles generated using either electrochemical technique 1 or method 2 have an inhibitory impact on a variety of microorganisms. Method 2's produced nano-Cr2O3 (41 nm) inhibits almost as well as the gold standard. Bacterial growth on agar plates is shown as a zone of inhibition. This proves that the recently produced Cr2O3 nanoparticles are effective antibacterial agents.

Table 7: Cr_2O_3 nanoparticles: Zone of inhibition (mm)

Test Organism	Escherichia Coli	Pseudomonas aregunosa
Cr_2O_3 (M1) (mm)	0.6	0.5
Cr_2O_3 (M2) (mm)	0.7	0.6
Standard/+^{ve}control (mm)	1.0	0.9

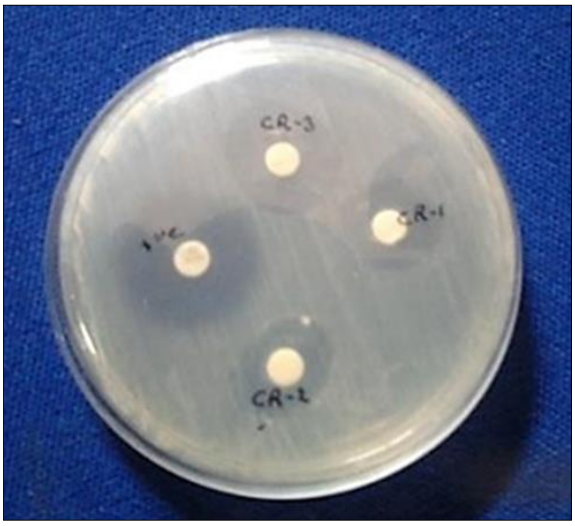

Fig 8: Zone of inhibition (mm) of Cr_2O_3 nanoparticles on *E. coli*

Reuse of catalyst

The Cr2O3 nanoparticles were reused so that the cost-effectiveness of the preparation procedure could be evaluated. When the KMnO4 was broken down, the solution was left undisturbed for roughly 8 hours before being decanted for its supernatant. After a thorough cleaning in double-distilled water, the catalyst was reactivated for further breakdown using a new KMnO4 solution. The findings indicate that the effectiveness of the decomposition method dropped by 20% when used twice. The catalyst's effectiveness decreased with continued usage.

Conclusion

According to the study, there are advantages to both biological and electrochemical approaches for producing metal oxide nanoparticles, and the benefits vary based on the specific needs of the application. Eco-friendliness and cost-effectiveness are the main advantages of biological synthesis, but electrochemical techniques offer more exact control over the shape and makeup of nanoparticles. The results of the characterisation demonstrate that both techniques yield nanoparticles with favourable characteristics like stability and a large surface area. This study provides insights into the selection of appropriate synthesis techniques based on particular applications in fields like electronics, environmental science, and biomedicine by comparing these approaches. The results highlight the possibility of integrating the two techniques to create hybrid synthesis strategies that leverage the advantages of each methodology.

References

1. Nguyen DD, Lai J-Y. Synthesis, bioactive properties, and biomedical applications of intrinsically therapeutic nanoparticles for disease treatment. Chem Eng J,2022:435:134970.
2. Bharathala S, Sharma P. Chapter 8—Biomedical applications of nanoparticles. In: Maurya PK, Singh S, editors. Nanotechnology in modern animal biotechnology. Amsterdam: Elsevier, 2019, 113–32.
3. Yaqoob AA, Ahmad H, Parveen T, Ahmad A, Oves M, Ismail IMI, *et al*. Mohamad Ibrahim MN. Recent advances in metal decorated nanomaterials and their various biological applications: A review. Front Chem,2020:8:341.
4. Nadaf SJ, Jadhav NR, Naikwadi HS, Savekar PL, Sapkal ID, Kambli MM, *et al*. Green synthesis of gold and silver nanoparticles: Updates on research, patents, and future prospects. OpenNano,2022:8:100076.
5. Yaduvanshi N, Jaiswal S, Tewari S, Shukla S, Wabaidur SM, Dwivedi J, *et al*. Palladium nanoparticles and their composites: Green synthesis and applications with special emphasis to organic transformations. Inorg Chem Commun,2023:151:110600.
6. Paiva-Santos AC, Herdade AM, Guerra C, Peixoto D, Pereira-Silva M, Zeinali M, *et al*. Plant-mediated green synthesis of metal-based nanoparticles for dermopharmaceutical and cosmetic applications. Int J Pharm,2021:597:120311.
7. Nguyen NTT, Nguyen TTT, Nguyen DTC, Tran TV. Green synthesis of ZnFe2O4 nanoparticles using plant extracts and their applications: A review. Sci Total Environ,2023:872:162212.
8. Nasaruddin RR, Chen T, Yao Q, Zang S, Xie J. Toward greener synthesis of gold nanomaterials: From biological to biomimetic synthesis. Coord Chem Rev,2021:426:213540.
9. Erdogan O, Abbak M, Demirbolat GM, Birtekocak F, Aksel M, Pasa S, Cevik O. Green synthesis of silver nanoparticles via Cynara scolymus leaf extracts: The characterization, anticancer potential with photodynamic therapy in MCF7 cells. PLoS ONE, 2019, 14. doi: 10.1371/journal.pone.0216496.
10. Tyagi PK, Quispe C, Herrera-Bravo J, Tyagi S, Barbhai MD, Kumar M, *et al*. Synthesis of silver and gold nanoparticles: Chemical and green synthesis method and its toxicity evaluation against pathogenic bacteria using the ToxTrak test. J Nanomater,2021:2021:3773943.
11. Hasan A, Morshed M, Memic A, Hassan S, Webster TJ, Marei HE. Nanoparticles in tissue engineering: Applications, challenges and prospects. Int J Nanomed,2018:13:5637–55.
12. Zheng X, Zhang P, Fu Z, Meng S, Dai L, Yang H. Applications of nanomaterials in tissue engineering. RSC Adv,2021:11:19041–58.
13. Upadhyay LSB, Rana S, Kumar N. Chapter 20—Nanomaterials in tissue engineering: Applications and challenges. In: Das Talukdar A, Dey Sarker S, Patra JK, editors. Advances in nanotechnology-based drug delivery systems. Amsterdam: Elsevier, 2022, 533–54.
14. Habibzadeh F, Sadraei SM, Mansoori R, Singh Chauhan NP, Sargazi G. Nanomaterials supported by polymers for tissue engineering applications: A review. Heliyon, 2022, 8.
15. Fathi-Achachelouei M, Knopf-Marques H, Ribeiro da Silva CE, Barthès J, Bat E, Tezcaner A, Vrana NE. Use of nanoparticles in tissue engineering and regenerative medicine. Front Bioeng Biotechnol,2019:7:113.
16. Eivazzadeh-Keihan R, Bahojb Noruzi E, Khanmohammadi Chenab K, Jafari A, Radinekiyan F,

Hashemi SM, *et al*. Metal-based nanoparticles for bone tissue engineering. J Tissue Eng Regen Med,2020:14:1687–714.
17. Gobi R, Ravichandiran P, Babu RS, Yoo DJ. Biopolymer and synthetic polymer-based nanocomposites in wound dressing applications: A review. Polymers,2021:13:1962.
18. Radulescu DM, Neacsu IA, Grumezescu AM, Andronescu E. New insights of scaffolds based on hydrogels in tissue engineering. Polymers,2022:14:799.
19. Ehtesabi H, Fayaz M, Hosseini-Doabi F, Rezaei P. The application of green synthesis nanoparticles in wound healing: A review. Mater Today Sustain,2023:21:100272.
20. Mujahid MH, Upadhyay TK, Khan F, Pandey P, Park MN, Sharangi AB, *et al*. Metallic and metal oxide-derived nanohybrid as a tool for biomedical applications. Biomed Pharmacother,2022:155:113791.